

LETTERS

No oceans on Titan from the absence of a near-infrared specular reflection

R. A. West¹, M. E. Brown², S. V. Salinas³, A. H. Bouchez⁴ & H. G. Roe²

With its substantial atmosphere of nitrogen, hydrocarbons and nitriles, Saturn's moon Titan is a unique planetary satellite. Photochemical processing of the gaseous constituents produces an extended haze that obscures the surface. Soon after the Voyager fly-bys in 1980 and 1981 photochemical models^{1–3} led to the conclusion that there should be enough liquid methane/ethane/nitrogen to cover the surface to a depth of several hundred metres. Recent Earth-based radar echoes imply that surface liquid may be present at a significant fraction of the locations sampled⁴. Here we present ground-based observations (at near-infrared wavelengths) and calculations showing that there is no evidence thus far for surface liquid⁵. Combined with the specular signatures from radar observations, we infer mechanisms that produce very flat solid surfaces, involving a substance that was liquid in the past but is not in liquid form at the locations we studied.

Specular reflection from a surface that is smooth on the scale of the wavelength of the observation can be used to diagnose surface liquid. We searched for specular reflection in high-resolution images of Titan obtained on 20 nights between 17 September 2003 and 11 January 2004, and 11 nights between 2 September 2004 and 3 November 2004. On the four nights of 24–27 December 2004 we observed Titan continuously for approximately ten hours each night, allowing a much more precise search for changing specular reflection. We scaled the intensity of each image relative to the others by scaling to the brightness of the outer edge of the northern limb of Titan, which is only affected by the relatively unchanging haze and not by clouds or surface features.

No specular reflection is obvious in visual inspection of any of the images. The locations sampled in these images are shown in Fig. 1. To search for fainter specular reflection in the extensive December 2003 images, we projected each image onto a cylindrical latitude–longitude map to examine the change in surface brightness of individual locations on the surface of Titan with time as Titan rotated. These differential phase curves for the four regions that could have shown specular reflection are shown in Fig. 2.

To understand how sensitive the near-infrared images are for the detection of a specular signature, we simulated the radiative transfer of photons scattered from Titan's haze and surface. To produce these calculations we modified a public-domain code⁶ to compute the intensity. The code includes multiple scattering from a plane-parallel multilayer haze and scattering from a surface with a Lambert (isotropic) reflection model. Our modification follows a formalism for the optical properties of a distribution of wave slopes and facet orientations used by the terrestrial sea-surface community⁷. Multiple surface–atmosphere reflections are included just as they are for a Lambert surface. Accuracy to better than 1% was verified by comparison with a benchmark calculation (H. Gordon, personal communication, 1994).

Campbell *et al.*⁴ report a specular signature at 12 of the 16 locations they sampled with the Arecibo radar. For these they derived root-mean-square (r.m.s.) slope values between 0.5 and 3.5 degrees with a median value of ~2 degrees and uncertainty typically 20% of the mean value. In this work we calculated the specular signature for r.m.s. slope values of 3.1, 4.9 and 5.5 degrees. The results are shown in Fig. 3 for these three r.m.s. slope values and for two wavelengths (2.1 and 0.938 μm) with appropriate differences in haze optical depth and scattering asymmetry parameter. In terms of I/F , where I is the reflected intensity and πF is the incident solar flux, the specular signature (the peak at the centre of the disk) has a full-width at half-maximum (FWHM) value of about 5.5% of Titan's diameter and a peak value of $I/F = 0.37$ for the case with optical depth $\tau = 0.3$ and r.m.s. slope 3.1 degrees. The FWHM is 11% of Titan's diameter and the maximum I/F is 0.15 for the higher r.m.s. slope value of 5.5 degrees. The signatures are weaker for the higher optical depth case

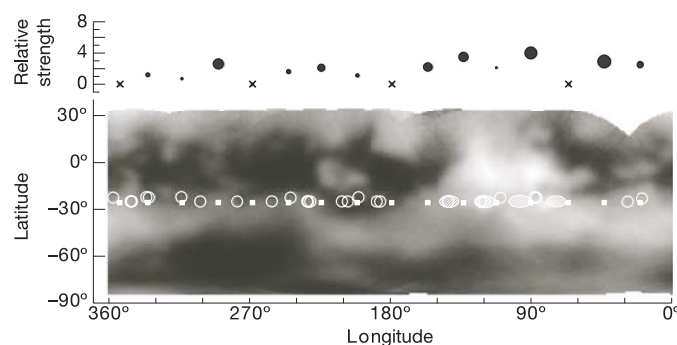


Figure 1 | A cylindrical projection map of Titan at 2- μm wavelength¹¹. The bright Xanadu region appears near the equator at 90 degrees longitude. The small solid squares show the location of the radar observations of ref. 4. The open circles show the region of expected specular reflection for our 27 Keck images. All observations were obtained with the Keck II adaptive optics system and NIRC2 near-infrared camera and spectrograph¹², with an angular resolution of approximately 0.049 arcsec at 2.1 μm , corresponding to a spatial resolution on Titan of between 300 and 400 km. On most nights we obtained a single set of three-position dithered 30-s exposures in the K' (1.95–2.30 μm) filter. No more than 15% of the area of the open circles could be covered with material with an r.m.s. smoothness comparable to that measured by radar. The hatched regions near 142, 119, 96 and 74 degrees longitude show the region covered by intensive Keck observations where the upper limits to specular reflection are even stronger. The upper panel shows the relative strength of the radar specular reflection, while the size of the symbol used shows approximately the size of the region from which the specular signature came and is proportional to the inferred r.m.s. slope. An 'x' means that no radar specular reflection was visible at that location.

¹MS 169-237 Jet Propulsion Laboratory, 4800 Oak Grove Drive, Pasadena, California 91109, USA. ²Division of Geological and Planetary Sciences, California Institute of Technology, Pasadena, California 91125, USA. ³Centre for Remote Imaging, Sensing and Processing, National University of Singapore, Blk SOC 1, Level 2, Lower Kent Ridge Rd, Singapore 119260. ⁴W. M. Keck Observatory, 65-1120 Mamalahoa Highway, Kamuela, Hawaii 96743, USA.

but the FWHM values are unchanged. The values quoted above apply to an observation (by the Cassini Visible and Infrared Mapping Spectrometer⁸, or VIMS) capable of fully resolving these features. The point-spread function of our ground-based images reduces the peak as shown in Fig. 3.

A specular reflection as strong as those calculated for the optical thickness at 2.1 μm would immediately be obvious in any of the Keck images. A surface that is composed of only a fractional covering of a smooth surface would have a smaller specular reflection, however. To place limits on the smooth surface fraction we added simulated specular reflections to each of the images and determined when the specular reflection was obvious in the image. For the median r.m.s. surface slopes found by Arecibo of ~ 2 degrees, we can firmly rule out smooth (at 2.1 μm) surfaces covering more than 15% of any of the 31 regions surveyed. A similar assessment for high-resolution Cassini VIMS images yields a limit of 2% for the same r.m.s. slope.

A stronger limit can be placed on the specular locations for the four nights of extensive observation. We again add simulated specular reflections to each image from those nights, but now quantitatively examine the brightness as a function of solar phase angle, with and without the specular reflection. For the r.m.s. surface slope 3.1-degree model, we place upper limits to the smooth fraction of the potential specular surface of 3, 8, 10 and 8% for the regions at 142, 119, 96 and 74 degrees longitude, respectively. A similar analysis of high-resolution Cassini VIMS images should provide tighter limits by about a factor of four.

The upper limits we place on the fraction of Titan's surface covered by liquid challenge the liquid-surface interpretation suggested by the Arecibo observations. It is possible that the radar observations sampled lakes of liquid hydrocarbons as small as several tens of kilometres in diameter that were not seen in the infrared images. Our results suggest that at most a small percentage of the surface of Titan studied thus far could be covered by lakes. Alternatively, we must ask what processes might form a surface that is sufficiently flat and smooth at a wavelength of 13 cm to produce the specular signatures seen in the Arecibo echoes, and which is at the same time rough enough to inhibit a specular signature at 2.1 μm . We propose three possible mechanisms: evaporite deposits, ponding of an inviscid fluid which then froze, and surface accumulation of sedimented haze from the stratosphere. All of these involve liquid on the surface at

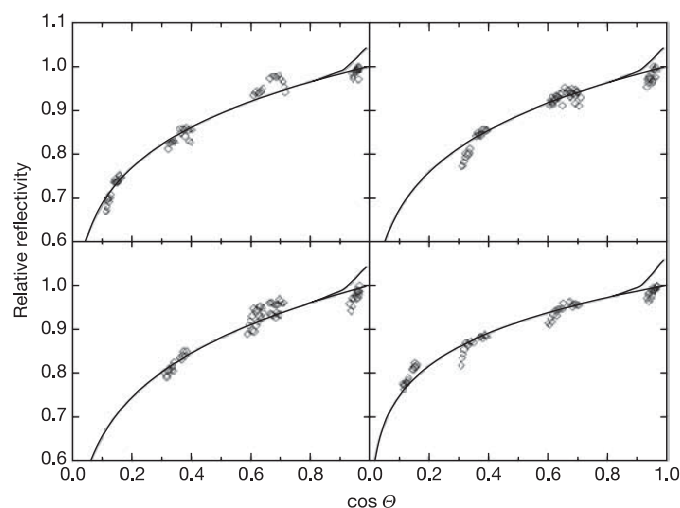


Figure 2 | The 2.1- μm brightness of four locations on the surface of Titan measured over four days as a function of solar zenith angle. The locations are at longitudes 142, 119, 96 and 74 degrees and are shown as hatched regions in Fig. 1. The relative intensities are fitted to a function of the form $\cos \theta$, where θ is the solar zenith angle. The small deviations from these lines near $\cos \theta = 1$ show the expected effect of adding a specular reflection at the stated upper limit and represent our detection limits.

some time in the past but not the present.

A fourth possibility sometimes considered—that a thin surface layer of solid particles is floating on a liquid—is problematic because (1) the density of a solid hydrocarbon or water ice particle is likely to be higher than that of liquid methane/ethane/nitrogen and (2) the surface tension of liquid methane is very low. The first of these difficulties could be overcome if the solid hydrocarbon were structured as a fluffy aggregate, which indeed the sedimenting particles are thought to be⁹.

Evaporite deposits on the Earth are a class of sedimentary minerals and sedimentary rocks that form by precipitation from evaporating

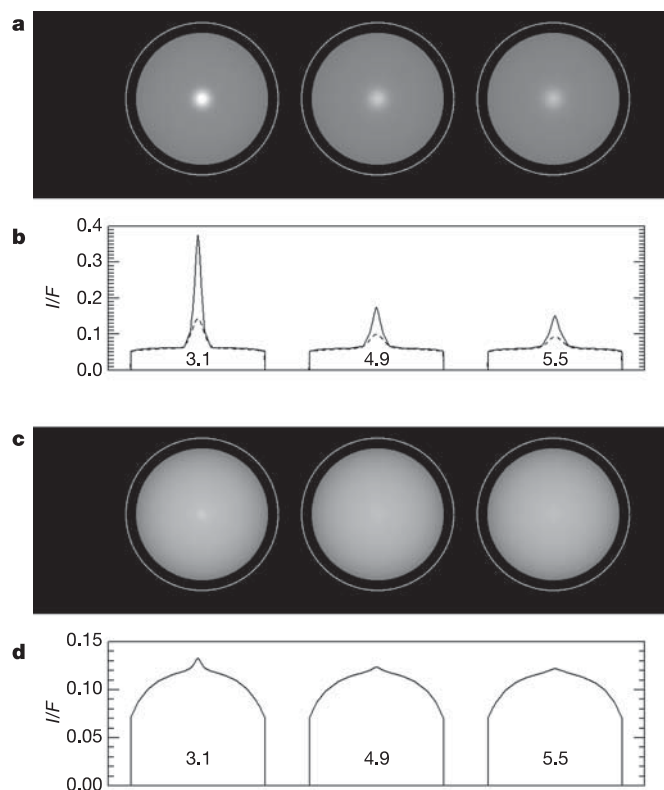


Figure 3 | Synthesized images and plots of reflectivity. The perspective is for Titan at opposition. The plots cut through the centre of each image. Panels **a** and **b** apply to the 2.1- μm window where the optical depth is close to 0.3 and the haze scattering asymmetry parameter is 0.2. The dashed curve was produced by convolving the synthetic image with the Keck point-spread function. The solid curves apply to Cassini 2.1- μm images near Titan where the spatial resolution is much better than 300 km. Panels **c** and **d** are for the Cassini Imaging Science Subsystem images in the 0.938- μm window where the optical depth is 3 and the haze asymmetry parameter is close to 0.75. Grey levels are calculated for view angles not more than 60 degrees to avoid errors near the limb from the plane-parallel approximation. The white circles surrounding the image show the location of the solid surface radius. The labels under the specular feature indicate the r.m.s. slope. Atmospheric scattering properties are determined by the nature of the haze particles. The optical depth of the haze may be as high as 3 at 0.938 μm , and close to 0.3 near 2.1 μm (ref. 13). We computed particle scattering phase functions and single-scattering albedos at 0.938 μm , based on a fractal aggregate model^{14,15} with optical constants of Titan 'tholin'¹⁶ at 0.938 μm but with the imaginary part multiplied by 4/3 to match the current geometric albedo measurements better. The derived optical depth at 2.1 μm (ref. 13) was also based on a fractal aggregate model with scattering phase function asymmetry (cosine-weighted angular distribution) $g = 0.2$. Results for 2.1 μm reported here used a Henyey-Greenstein phase function ($P(g, \theta) = (1 - g^2)/(1 + g^2 - 2g \cos \theta)^{3/2}$) with $g = 0.2$. The Fresnel reflection coefficients are derived from the complex refractive index of the liquid. We used a value of (1.286, 0.114) as representative for a mixture of liquid methane/ethane near 90 K (ref. 17).

fluid. Common terrestrial evaporite minerals are halite, gypsum and anhydrite, which can form as sea water evaporates, and the rocks limestone and dolostone. On Titan the composition would probably be a hydrocarbon layer from fully or partially dissolved and undissolved organic material that entered a liquid methane/ethane/nitrogen body from an accumulation of sedimenting organic haze or geothermal sources. If the evaporite material were porous it could contain a significant amount of subsurface liquid that would be available to replenish methane lost to photo-dissociation.

A second possible mechanism involves volcanic extrusion of liquid water/ammonia which ponded to form a very flat surface and then froze. This is less likely to be the mechanism producing the Arecibo echoes, however, because the radar cross-sections are more consistent with organic material. This objection may be overcome by a surface deposit of organic sediment, a specific example of our next proposal.

A third possibility is that deposits of organic haze over geologic timescales have filled in topographically low areas with a flat top facilitated by liquid methane/ethane/nitrogen that later evaporated, or by wind action. These deposits may well be porous and contain significant amounts of subsurface liquid methane/ethane/nitrogen that now buffers the atmosphere.

Although this possibility and the other mechanisms we propose may succeed in accounting for a solid surface smooth enough to produce a specular signature at 13 cm, we point out that any solid surface will roughen at 13-cm scales over geologic time owing to a variety of geologic or aeolian (wind-related) processes, and so we may need to invoke a geologically young age as well as one of these mechanisms to explain the surfaces we see.

In addition, current large-scale cloud activity on Titan is rare outside the southern high latitudes but is predicted to move north as Titan's southern summer turns to southern autumn¹⁰, suggesting the possibility that these regions are seasonally refreshed with precipitation, which could work to smooth the surface. Unless there is a subsurface reservoir capable of sustaining atmospheric methane, the long-term prognosis is for a Titan atmosphere depleted in methane, having profound implications for photochemistry, radiative balance and circulation.

Received 10 February; accepted 18 May 2005.

1. Flasar, F. M. Oceans on Titan. *Science* **221**, 55–57 (1983).

2. Lunine, J. I., Stevenson, D. J. & Yung, Y. L. Ethane ocean on Titan. *Science* **222**, 1229–1230 (1983).
3. Yung, Y. L., Allen, M. & Pinto, J. P. Photochemistry of the atmosphere of Titan: Comparison between model and observations. *Astrophys. J. Suppl.* **55**, 465–506 (1984).
4. Campbell, D. B., Black, G. J., Carter, L. M. & Ostro, S. J. Radar evidence for liquid surfaces on Titan. *Science* **302**, 431–434 (2003).
5. Porco, C. C. *et al.* Imaging Titan from the Cassini Spacecraft. *Nature* **434**, 159–168 (2005).
6. Evans, K. F. & Stephens, G. L. A new polarized radiative transfer model. *J. Quant. Spectrosc. Radiat. Trans.* **46**, 413–423 (1991).
7. Deuze, J. L., Herman, M. & Santer, R. Fourier series expansion of the transfer equation in the atmosphere-ocean system. *J. Quant. Spectrosc. Radiat. Trans.* **41**, 483–494 (1989).
8. Brown, R. H. *et al.* The Cassini Visual and Infrared Mapping Spectrometer (VIMS) investigation. *Space Sci. Rev.* **115**, 111–168 (2004).
9. West, R. A. & Smith, P. H. Evidence for aggregate particles in the atmospheres of Titan and Jupiter. *Icarus* **90**, 330–333 (1991).
10. Brown, M. E., Bouchez, A. H. & Griffith, C. A. Direct detection of variable tropospheric clouds near Titan's south pole. *Nature* **420**, 795–797 (2002).
11. Bouchez, A. H., Brown, M. E., Schaller, E. L. & Roe, H. G. Cloud frequency and wind speed in Titan's troposphere. *Bull. Am. Astron. Soc.* **36**, 1696 (2004).
12. Wizinowich, P. *et al.* Performance of the W.M. Keck observatory natural guide star adaptive optic facility: the first year at the telescope. *Proc. SPIE* **4007**, 2–13 (2000).
13. Gibbard, S. G. *et al.* Titan's 2 μ m surface albedo and haze optical depth in 1996–2004. *Geophys. Res. Lett.* **32**, L17S02 (2004).
14. Lemmon, M. T. *Properties of Titan's Haze and Surface*. PhD thesis, Arizona Univ. (1994).
15. Grieger, B., Lemmon, M. T., Markiewicz, W. J. & Keller, H. U. Inverse radiation modeling of Titan's atmosphere to assimilate solar aureole imager data of the Huygens probe. *Planet. Space Sci.* **51**, 147–158 (2003).
16. Khare, B. N. *et al.* Optical constants of organic tholins produced in a simulated Titanian atmosphere—from soft-x-ray to microwave-frequencies. *Icarus* **60**, 127–137 (1984).
17. Martonchik, J. V. & Orton, G. S. Optical constants of liquid and solid methane. *Appl. Opt.* **33**, 8306–8317 (1994).

Acknowledgements We benefited from radiative transfer benchmark calculations provided by H. Gordon and from discussions with D. Campbell, R. Lorenz and S. Ostro. Part of this work was performed by the Jet Propulsion Laboratory, California Institute of Technology under contract with the National Aeronautics and Space Administration.

Author Contributions M.E.B., A.H.B. and H.G.R. supplied the Keck observations and data analysis. S.V.S. provided the light-scattering model calculations.

Author Information Reprints and permissions information is available at npg.nature.com/reprintsandpermissions. The authors declare no competing financial interests. Correspondence and requests for materials should be addressed to R.A.W. (Robert.A.West@jpl.nasa.gov).